13th World Conference on Earthquake Engineering
Vancouver, B.C., Canada
August 1-6, 2004
Paper No. 228

INVESTIGATION OF JACOBSEN'S EQUIVALENT VISCOUS DAMPING APPROACH AS APPLIED TO DISPLACEMENT-BASED SEISMIC DESIGN

Hazim DWAIRI[1] and Mervyn KOWALSKY[2]

SUMMARY

This paper discusses the approximation of the maximum displacement of nonlinear hysteretic systems through the use of an equivalent linear system with effective properties (i.e. reduced stiffness and equivalent viscous damping). Because of its simplicity in application, this concept has been widely utilized in the displacement-based seismic design procedure. This paper aims to investigate the accuracy and potential problems associated with the equivalent viscous damping concept as applied to direct displacement-based seismic design, and to suggest a modification to Jacobsen's approach that is based on ground motion characteristics. The parameters considered include: Earthquake time history (reversal and fling-type events), hysteretic models ranging from origin centered systems to Takeda-type response systems. Results of the research indicate that the fundamental period of the ground motion is a critical variable in assessing the accuracy of the equivalent viscous damping concept. In general, results from non-linear analysis conducted with regular sinusoidal events is excellent, which is expected given the assumptions of sinusoidal response in the equivalent viscous damping approach, however, results from real time histories indicate more scatter. Recommendations for the use of the equivalent viscous damping approach in direct displacement-based seismic design are presented for SDOF system based on the results of 100 earthquake records and 95,000 inelastic time history analyses.

INTRODUCTION

Direct displacement-based seismic design (DDBD) focuses the design directly on displacement demand which is more attractive than strength as a damage measure. Due to the fact that structures in seismic regions are designed to respond in-elastically and the design procedure needs to be simple, methods of approximating maximum displacement of inelastic system gain primary importance in DDBD.

One of the methods used to determine the maximum displacement of a non-linear system is the inelastic response spectrum, where an exact spectrum could be obtained for a SDOF system with a selected period and hysteretic rule. Unfortunately, the resulting R-μ-T relationships vary also as a function of earthquake and soil type. The other method being used involves representing the nonlinear system by

[1]PhD Candidate. Department of Civil Engineering, North Carolina State University, Campus Box 7908, Raleigh NC-27695
[2]Assistant Professor, Department of Civil Engineering, North Carolina State University, Campus Box 7908, Raleigh NC-27695

an equivalent elastic system with equivalent stiffness and equivalent viscous damping. The advantage of this method lies in its simplicity and ability of using the more familiar elastic response spectrum.

The Equivalent viscous damping concept was first introduced by Jacobsen in 1930 [1]. In his paper, Jacobsen approximated the steady state solution of a nonlinear SDOF system by equating the energy dissipated by that system to the energy dissipated by one cycle of sinusoidal response of a linear system with equivalent viscous damping. He also pointed out the arbitrariness in choosing the one cycle criterion and that it is not better than the other criterion of equivalent time average of damping force, although he noted it was superior at or near resonance. In 1974, Gulkan and Sozen [2] introduced the definition of substitute damping, utilizing the earthquake time history and the response time history of SDOF frames. In their research, they computed the substitute viscous damping by equating the energy input into the system to the energy dissipated by an imaginary viscous damper over the period of excitation. Gulkan and Sozen compared the results of their approach with experimental results and with Jacobsen's approach, and found them to be in good agreement. It should be noted that the Gulkan and Sozen approach requires prior knowledge of the system response which is not available at the design stage, while Jacobsen's approach requires no such knowledge and as a result is more appealing for design procedures.

In 1965, Hudson [3] investigated the equivalent viscous damping approach for hysteretic systems, he concluded that the maximum possible value of the equivalent viscous damping for bilinear systems is 15.9% and most hysteretic systems have values less than that. In his derivation he assumed a bilinear model with initial stiffness K_0, secondary stiffness rK_0, yield displacement D_y and maximum displacement D_m as shown in figure 1.

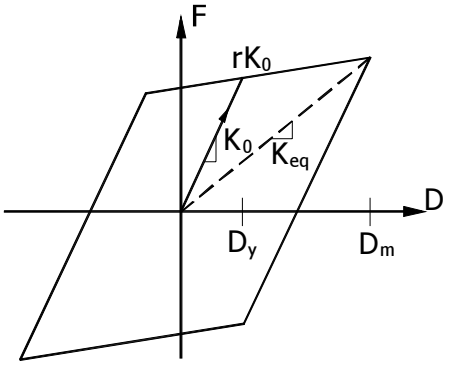

Figure 1. Bilinear Hysteretic Model

Hudson then equated the energy dissipated by one cycle (i.e area of the bilinear loop) with that dissipated by spring-dashpot-mass system at resonance with a spring constant K_0 and viscous damping ξ_{eq}. The resulted equation was in the form:

$$\xi_{eq} = \frac{2}{\pi}\frac{(\mu-1)(1-r)}{\mu^2} \tag{1}$$

In 1976, Shibata and Sozen [4] introduced the definition of a substitute structure to determine the seismic design forces for a given structure and earthquake intensity. They characterized the substitute structure by the substitute damping and effective, or secant stiffness to maximum response. This is the slope of the line that connects the origin to the maximum displacement in a hysteretic model. Utilizing the definition of effective stiffness, and applying it to the bilinear hysteretic model in figure 1 leads to the following relation between initial and effective stiffness:

$$K_0 = \frac{\mu}{r\mu - r + 1} K_{eq} \tag{2}$$

In 1995, Kowalsky *et. al* [5] applied Jacobsen's approach to the Takeda hysteretic model [7]; by utilizing the same formulation and applying it to the bilinear hysteretic model shown in figure 1, i.e equating the energy dissipated by one cycle of the bilinear model with the energy dissipated by one cycle of sinusoidal response of a spring-dashpot-mass system at resonance, with spring constant K_{eq} yields:

$$\xi_{eq} = \frac{2}{\pi}\frac{(\mu-1)(1-r)}{\mu(1+r\mu-r)} \tag{3}$$

In 1980, Iwan [6] obtained optimal values for period shift and equivalent damping ratio based on statistical analysis of 12 earthquake records as follows:

$$\xi_{eq} = 0.0587(\mu-1)^{0.371} \tag{4}$$

A plot of the previous equations 1, 2 and 3 for different values of ductility is shown in figure 2. The bilinear factor r was taken equal to 0 (i.e elastic perfectly plastic loop). It is noted that Jacobsen's approach, which is based on equating the energy dissipated by one cycle to the energy dissipated by viscous linear system with effective stiffness, produces the highest value amongst the three methods and produces the maximum expected value of equivalent viscous damping that is 64% for elastic perfectly plastic system. On the other hand, Hudson's method, which is based on equating the energy dissipated by one cycle to the energy dissipated by viscous linear system with initial stiffness, produces a maximum value of 15.9%. The values produced by Iwan are less that those produced by the Hudson's method up to ductility value of 4; it worth mentioning that Iwan's and Jacobsen's equations keep increasing with ductility while Hudson's reaches a maximum then starts to decrease.

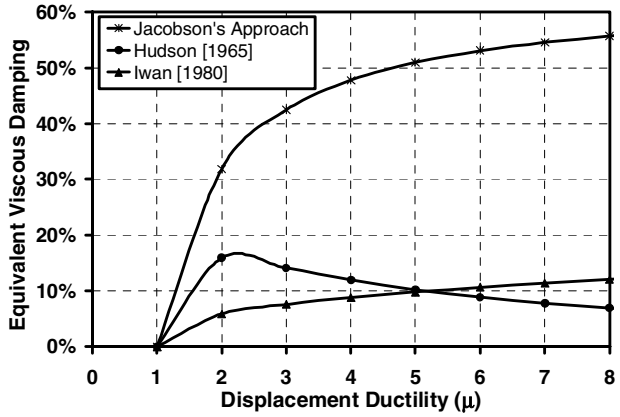

Figure 2. Comparison of Equivalent Viscous Damping

In this paper, an assessment algorithm has been used to investigate the accuracy of the equivalent viscous damping approach (Kowalsky's formulation of Jacobsen's approach [5]) as it's been used in direct displacement-based seismic design (DDBD). Jacobsen's approach was tested first for a sinusoidal earthquake to eliminate the main assumption in his approach. Then it was tested for real earthquake records, and finally a comprehensive evaluation of the approach was carried out utilizing a large number of earthquake records.

DIRECT DISPLACEMENT-BASED DESIGN REVIEW

Direct Displacement-Based Design aims to design a structure to achieve a selected target displacement using equivalent elastic system properties and elastic response spectrum generated for different damping values. The basic steps of this procedure as described by Kowalsky *et. al* [5] are:

1. **Obtain a target displacement:** In the case of a single column bridge, the target displacement can be obtained from the drift ratio or strain criterion that defines the desired level of performance of the column.

2. **Estimate level of equivalent viscous damping:** Using the chosen target displacement and an estimated yield displacement, the ductility level is calculated. Then it's used to calculate the hysteretic damping expected. The ductility versus hysteretic damping relationship is obtained utilizing Jacobsen's approach with a convenient assumed hysteretic model. An additional 0%-5% viscous damping could be added to obtain the level of equivalent viscous damping. This process is shown in figure 4, for a ductility of 2.1 and Takeda smallest loop model, a 10% equivalent viscous damping is estimated.
3. **Determine effective period of the structure:** utilizing the target displacement, level of damping and elastic response spectra for the chosen seismic demand, the equivalent period of the structure could be determined as shown in figure 5. For a design displacement of 0.375 m and 10% level of damping the equivalent period is estimated to be 2.1 seconds.
4. **Evaluate equivalent stiffness and design base shear:** using the equivalent period and the structure mass, the equivalent stiffness could be easily calculated. Compute the base shear by multiplying the equivalent stiffness by the design displacement.
5. **Design the structure:** and check for the assumed or estimated yield displacement, if it changes significantly, repeat the previous steps until convergence is achieved.

STUDY PARAMETERS AND ASSESSMENT ALGORITHM

In this study, The Takeda hysteretic model [7] and Ring-Spring hysteretic model [8] were considered as shown in figure 3. An expression between displacement ductility and hysteretic damping could be obtained by applying Jacobsen's approach to both models. The expression given by equations 5-7 is for the Takeda model, where μ is the displacement ductility, α is the unloading stiffness and γ is the reloading stiffness. Two extreme cases were selected for the Takeda model: the smallest and largest loop possible by changing α and β values. For the Ring-Spring model only the largest possible loop was considered and the equivalent viscous damping expression is not shown due to size limitations.

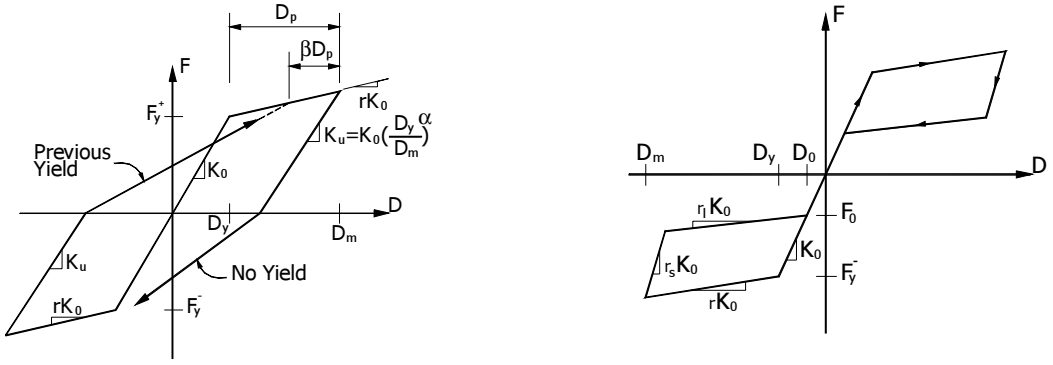

Figure 3. (a) Modified Takeda Hysteretic Model (b) Ring-Spring Hysteretic Model

$$\xi_{hyst} = \frac{2}{\pi} R_{LA} \tag{5}$$

$$R_{LA} = 1 - \frac{3}{4}\mu^{\alpha-1}\gamma - \frac{1}{4}\left[\frac{r\beta\mu}{\gamma}\left(1-\frac{1}{\mu}\right)+1\right]\left[2-\beta\left(1-\frac{1}{\mu}\right)-\mu^{\alpha-1}\gamma\right] - \frac{1}{4}\left[\frac{r\beta^2\mu}{\gamma}\left(1-\frac{1}{\mu}\right)^2\right] \tag{6}$$

$$\gamma = r\mu - r + 1 \tag{7}$$

Figure 4, shows a plot of the relationship between displacement ductility and hysteretic damping for the two extreme cases of Takeda's model and the Ring-Spring model. For the Takeda model, the maximum hysteretic damping produced by the largest loop is 41% and by the smallest is 32%, at impractical levels of ductility, while the largest damping level could be achieved by the Ring-Spring models is 12%. So in this study the hysteretic damping considered, ranges from 2% to 30%.

The major assumptions made by Jacobsen were (1) assuming a steady state response (sinusoidal) and, (2) the arbitrary choice of the one cycle criterion where Jacobsen utilizes only one cycle of the response to estimate the equivalent viscous damping. Those two assumptions play a major rule in the accuracy of the method especially if applied to real earthquake records. For instance, in a real earthquake response there is a good possibility that the maximum response will occur before the transient response damps and the system reaches a steady state response. In a fling type event, where the structure could be pushed immediately into the inelastic range forming one large loop, it seems reasonable to adopt the one cycle criterion, but what if the structure was pushed gradually into the inelastic range? In order to answer those questions, it was decided to investigate the accuracy of Jacobsen's approach for different types of ground motions.

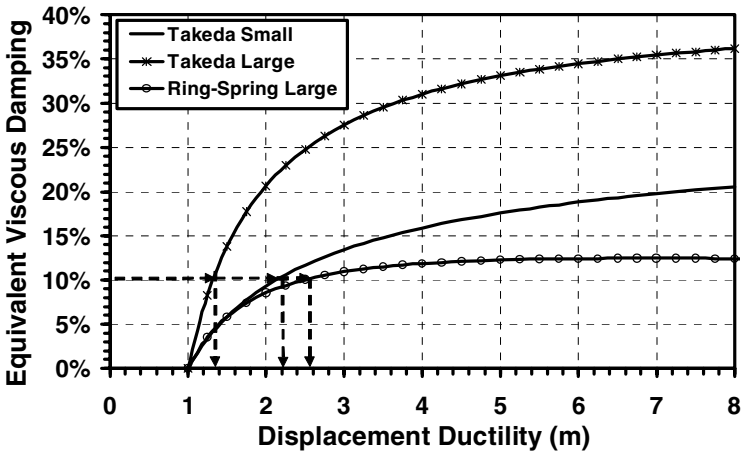

Figure 4. Hysteretic Damping versus Ductility for Modified Takeda and Ring-Spring Models

Direct displacement-based seismic design aims to design a structural system for a prescribed target displacement for a given earthquake intensity characterized by linear response spectra generated for various levels of viscous damping. The equivalent viscous damping is an important component of DDBD as it represents the non-linear response of the hysteretic system with the effective stiffness. The following algorithm has been used to investigate the accuracy of those relationships as they were used in the direct displacement-based seismic design.

1. Select earthquake time history and generate elastic response spectrum for different levels of damping. Each point maybe assumed to represent a SDOF equivalent oscillator with equivalent parameters, namely: design displacement, equivalent period and equivalent viscous damping, as shown in figure 5.
2. Select a hysteretic model, and formulate the relationship between ductility and equivalent viscous damping. Using the damping value from point one, the level of ductility in the system could be determined as shown in figure 4. For each level of hysteretic damping there are three values of ductility based on the modified Takeda and Ring-Spring hysteretic models.
3. Using the design displacement, ductility and equivalent period, define the inelastic SDOF structure by calculating, the initial stiffness and the yield moment of that structure.

4. Conduct inelastic time history analysis for the nonlinear structure and compare the maximum resulted displacement with the design displacement selected in point 1.

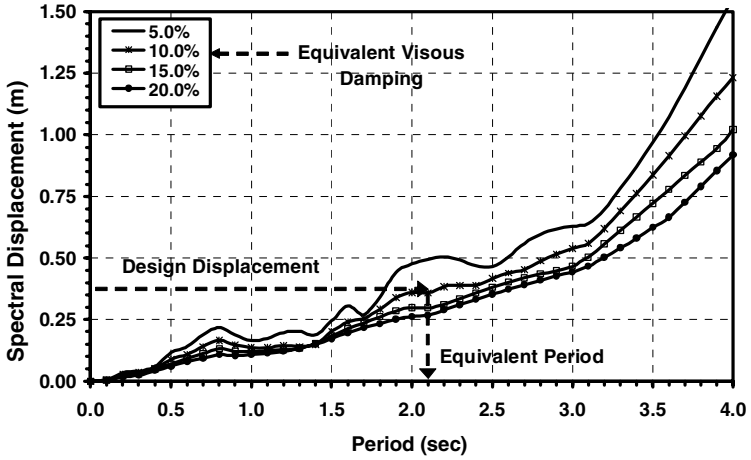

Figure 5. Equivalent SDOF Structure Definition, Tabas Elastic Displacement Spectra

ANALYSIS RESULTS AND DISCUSSION

In this paper, all the analyses were conducted assuming 2% viscous damping and different levels of hysteretic damping. The main focus of the analysis was to compare the chosen design displacement with the actual time history displacement and to use the ratio of both displacements as an estimate of the accuracy of the Jacobsen's approach. In the following sections are the results from the assessment of the equivalent viscous damping approach for various types of earthquakes.

Sinusoidal Earthquake Results

Since Jacobsen assumed a sinusoidal response in his formulation of the equivalent viscous damping, a number of sine waves were chosen to test the accuracy of the procedure based on the previous algorithm, only the results of one sine wave with circular frequency of 10 Hz is shown in figure 6. Elastic response spectra were generated for different viscous damping values ranging between 4% and 32%; assuming in the analysis 2% viscous damping and the remainder as hysteretic damping. Figure 6 shows the ratio of the inelastic time history analysis displacement to the design displacement (i.e inelastic oscillator to equivalent elastic oscillator displacement) versus equivalent period as a function of damping for the Takeda small and large loop models and Ring-Spring model. The dashed vertical line at a period of 0.62 seconds represents the period of the sinusoidal earthquake, and it is clear that it forms a turning point in the results. For periods less than the earthquake fundamental period the design is conservative (i.e overestimating the actual displacement) while for greater periods, the design generally underestimates the actual displacement. The same behavior was noticed for different sinusoidal earthquakes with different fundamental periods. Clearly Jacobsen's approach fails to estimate the maximum displacements for periods less than the earthquake period and high levels of damping.

The difference between the largest and smallest loop models is that the latter predicts less hysteretic damping for the same level of ductility. From figure 6, it's clear that the largest loop model overestimates the damping, which underestimates the displacements and yields more unconservative designs than the smallest loop model. Similarly, Ring-Spring model predicts the lowest damping for the same ductility which resulted in better ratios than both Takeda models.

To further investigate this behavior, the displacement time histories for the nonlinear and the equivalent linear oscillator were plotted as shown in figure 7. In addition, the hysteretic behavior for the nonlinear oscillator was also plotted with the linear response of the equivalent oscillator. Three oscillators were chosen to represent the results with ratios less than, equal to and greater than one. Each oscillator has a different fundamental period, effective and initial stiffness, ductility and equivalent viscous damping. It was concluded that for the cases with a ratio less than one, as shown in figure 7a, the displacements were overestimated because the nonlinear oscillator didn't respond in-elastically; instead it remained linear in most of the cases or did not go far into the inelastic range in other cases.

In the case where the ratio is nearly one, there was good agreement between the nonlinear and linear oscillator displacement time histories, the loops were developed gradually with sufficient amount of ductility into the system as shown in figure 7b.

After investigating some of the cases where the displacements were underestimated (i.e ratio greater than one), the hysteretic loops show a shift in the vibrating position of the nonlinear oscillator; this behavior is shown in figure 7c. This behavior is attributed to a large pulse that pushes the structure into the inelastic range and as a result, when it starts to unload, it vibrates around a new position which causes the shift in the loops as shown.

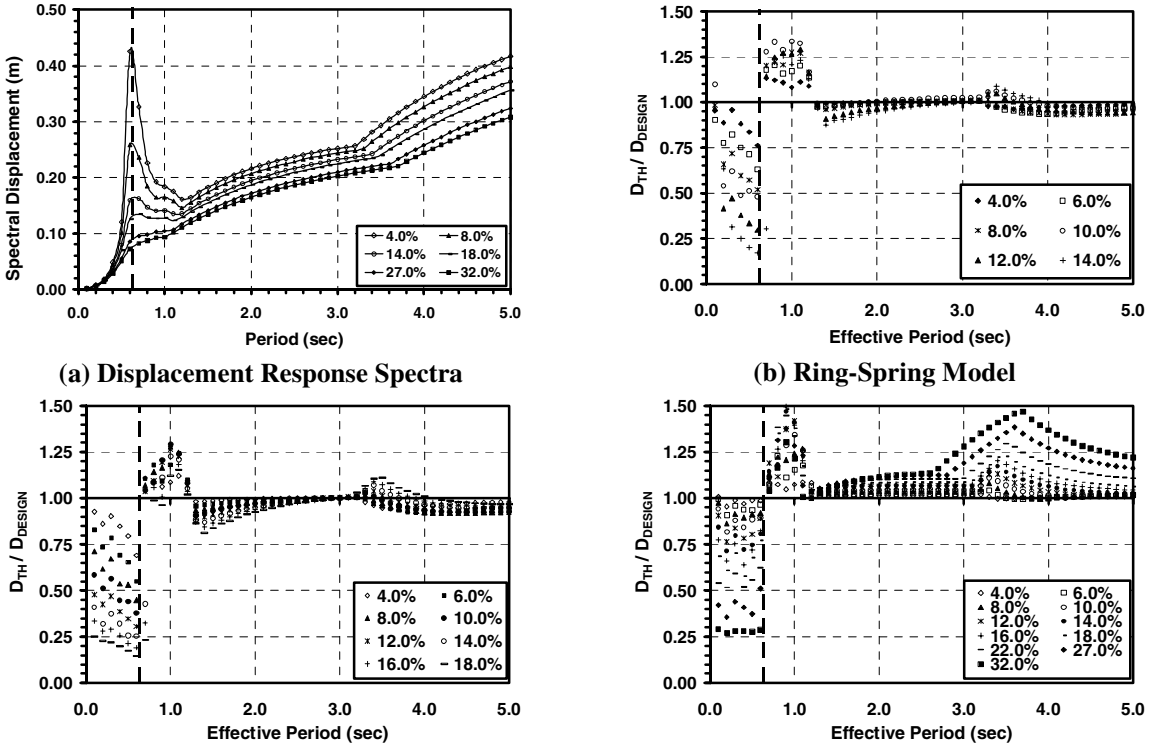

(a) Displacement Response Spectra

(b) Ring-Spring Model

(c) Takeda Small Loop Model

(d) Takeda Large Loop Model

Figure 6. Time-History to Design Displacement Ratio for Sinusoidal Earthquake (ω =10 Hz).

Typical Real Earthquake Results

Since real earthquake records are unlikely to have a specific frequency, but rather a range of frequencies, the sudden change in the results seen in figures 6 will be less apparent. Due to an expected increase in the scatter and to show a sample of real earthquakes results, three typical real earthquake records with different characteristics were selected: (1) Tabas 1978, (2) Kobe 1995, and (3) Northridge 1994. The ratio of inelastic time-history analysis displacement to design displacement (i.e inelastic

oscillator to equivalent elastic oscillator displacement) is shown in figures 8 through 10. The Takeda small and large loop models and Ring-Spring model were considered for various levels of damping.

The results from the three records show wider scatter than the sinusoidal earthquake, as expected, and varies between conservative and unconservative. For all records a wider scatter is noticed in the short period region where the oscillators vibrate about their fundamental frequency, while less scatter is noticed in the long period region where oscillators vibrate about the loading function frequency. The three records have distinctly different response spectrums; The Tabas record has a smoothly increasing spectrum while the other two have a flat portion or humps, depending on the level of damping. By comparing the results of all records, Jacbson's approach is not only sensitive to the earthquake characteristics but also to the oscillator fundamental period and level of ductility. Clearly the best way to quantify the scatter, in order to introduce any modification, will be through obtaining a large number of such results and utilizing a simple statistical analysis.

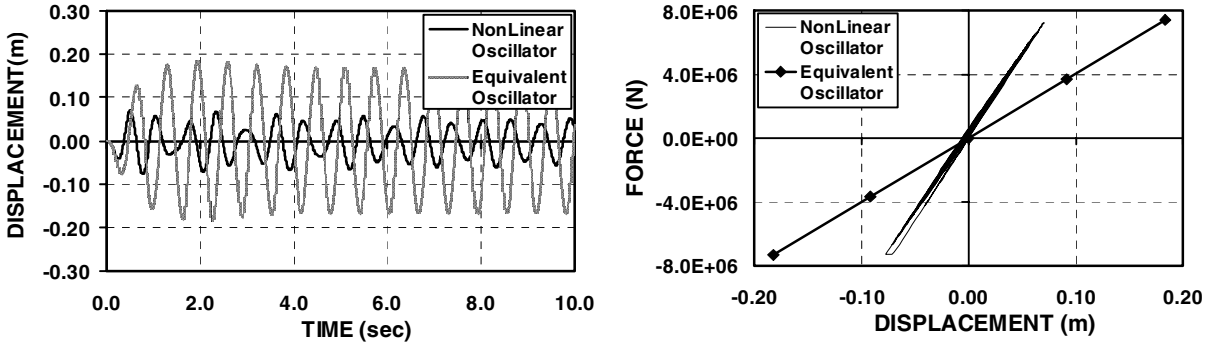

(a) Displacement Time-History and Hysteretic Behavior for Oscillator 1 (T_{eq}=0.7 sec)

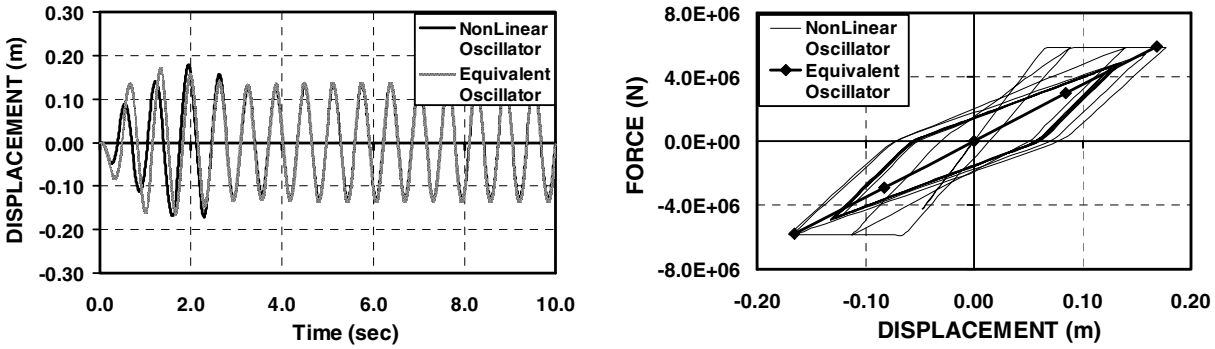

(b) Displacement Time-History and Hysteretic Behavior for Oscillator 2 (T_{eq}=0.75 sec)

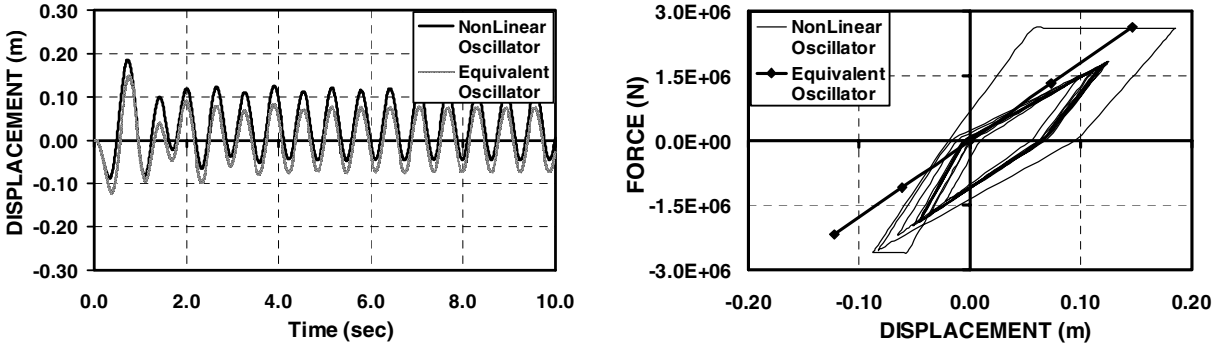

(c) Displacement Time-History and Hysteretic Behavior for Oscillator 3 (T_{eq}=1.05 sec)

Figure 7. Nonlinear and Equivalent Oscillators Displacement Time-History and Hysteretic Behavior for the Takeda Small Loop model, Sinusoidal Earthquake and 12% Hysteretic Damping

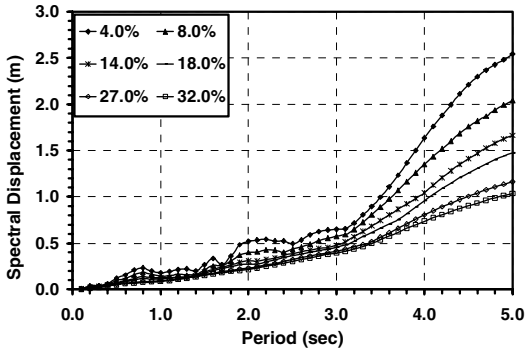

(a) Displacement Response Spectra

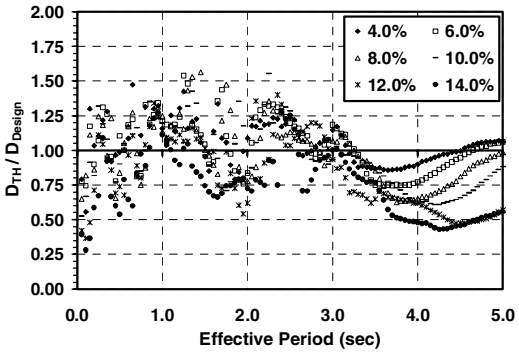

(b) Ring-Spring Model

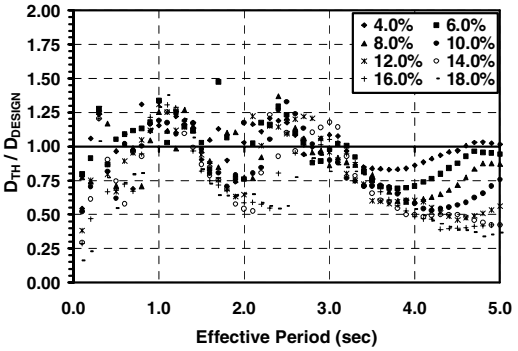

(c) Takeda Small Loop Model

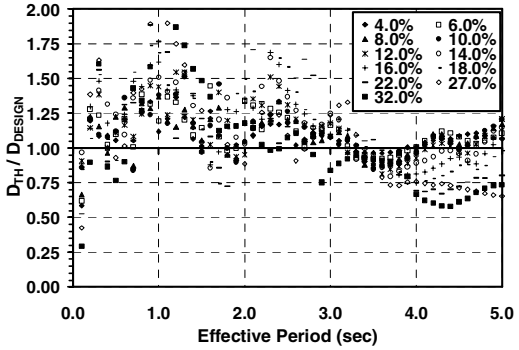

(d) Takeda Large Loop Model

Figure 8. Time-History to Design Displacement Ratio for the Tabas Earthquake, 1978.

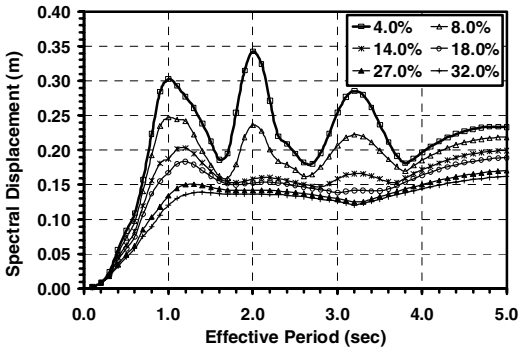

(a) Displacement Response Spectra

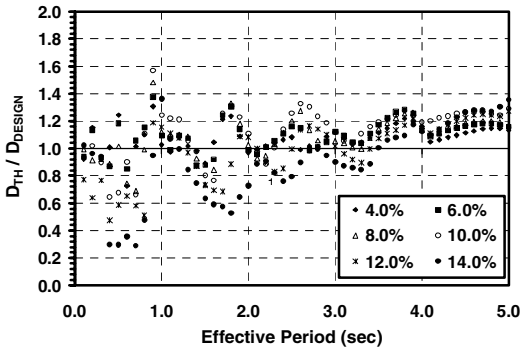

(b) Ring-Spring Model

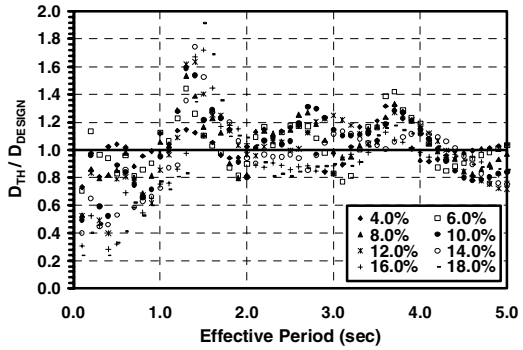

(c) Takeda Small Loop Model

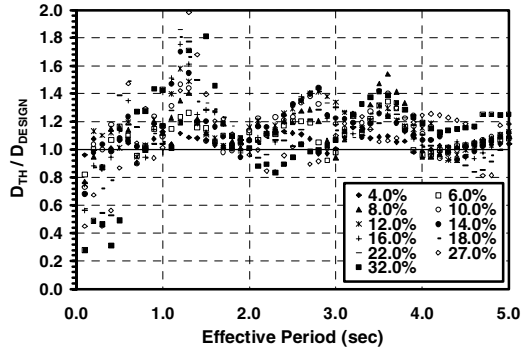

(d) Takeda Large Loop Model

Figure 9. Time History to Design Displacement Ratio for the Kobe Earthquake, 1995.

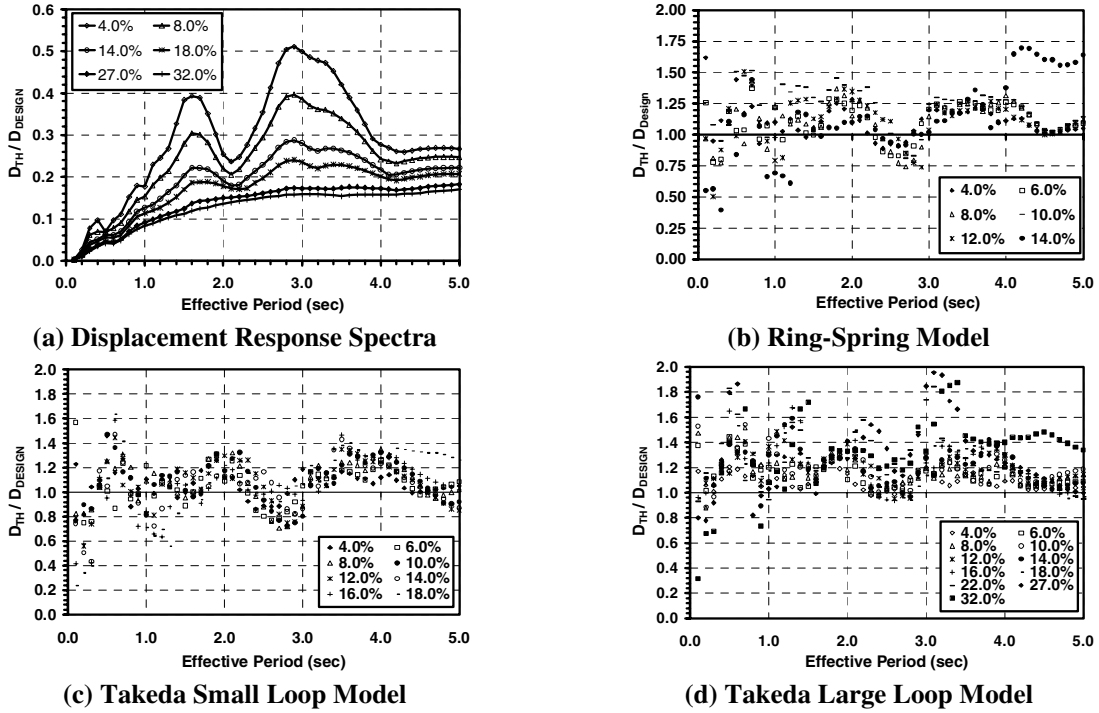

(a) Displacement Response Spectra

(b) Ring-Spring Model

(c) Takeda Small Loop Model

(d) Takeda Large Loop Model

Figure 10. Time History to Design Displacement Ratio for the Northridge Earthquake, 1994.

COMPREHENSIVE EVALUATION OF THE EQUIVALENT VISCOUS DAMPING APPROACH FOR TAKEDA HYSTERETIC MODEL

Given the variation of the results for real earthquakes and due to the significance of Jacobsen's approach in the direct displacement-based design, it was decided to evaluate the equivalent viscous damping approach for a large number of real earthquake records. In this study 100 earthquake records were selected, in order to evaluate the accuracy of Jacobsen's approach and to obtain more reliable and simple statistical data. The 100 records were collected and categorized based on the soil type, namely: B, C, D, E and NF by Miranda [9]. The previously discussed assessment algorithm was carried out for each one of the records, assuming the Takeda small and large loop models. 50 oscillators were used with fundamental periods range from 0.1 to 5.0 seconds, for the same levels of equivalent viscous damping shown in figures 8 through 10. Each oscillator was assumed to be designed using the DDBD approach and by following the steps, discussed previously in the assessment algorithm, the nonlinear oscillator was identified and inelastic time-history analysis was carried out to determine its actual maximum displacement. The total number of inelastic time-history analysis conducted in this part of the study is 95,000.

The results for each soil type (i.e 20 earthquake records), level of equivalent viscous damping and oscillator effective period were averaged and plotted with the coefficients of variation as shown in figures 11 through 14. Each point on those figures represents the average results of 20 earthquake records.

It is clearly noticed that both models are not conservative for most of the oscillators, except for very short effective periods. On average, and for the same level of equivalent viscous damping, the Takeda small loop model better estimates the oscillator maximum displacement than the Takeda large loop model. There is a slight difference between the results for the different soil types and the majority of the oscillators have a coefficient of variation bounded between 5% and 30%. By averaging all the results for each of figures 11 through 14, table 1 could be obtained.

Table 1. Average Time History to Design Displacement Ratio

Soil Type	Takeda Smallest Loop Hysteretic Model	Takeda Largest Loop Hysteretic Model
B	1.03	1.21
C	1.09	1.25
D	1.04	1.22
E	1.07	1.23
NF	1.01	1.18

At this stage of the research and based on the mean values shown in table 1, it is clear that the Takeda large loop model underestimates the design displacements with a factor of about 20% and in order to account for that, a reduction factor is needed to reduce the equivalent viscous damping estimated by the model. In the future a reduction factor will be introduced to equation 6, and this factor is expected to be a function of oscillator period, level of damping and earthquake characteristics.

CONCLUSIONS

Since the major assumption in Jacobsen's approach is a sinusoidal response, the approach was tested with a sinusoidal earthquake; the results indicated, as expected, that the approach works very well, however, it overestimates the displacements for periods less than the sine wave fundamental period. In some cases the approach underestimates the displacements not only due to overestimating damping but also due to the shift in the hysteretic loops because the oscillator starts vibrating around a new equilibrium position. A wider scatter is clearly noticed for real earthquake records, which varies based on the earthquake characteristics, oscillator fundamental period and level of ductility.

A comprehensive assessment of Jacobsen's equivalent viscous damping approach for Takeda hysteretic model was presented. 100 real earthquake records were used in the study, categorized base on the soil type; hysteretic damping levels between 2% and 30% were considered with additional 2% viscous damping and oscillator periods ranged between 0.1 to 5.0 seconds.

The results from the 100 earthquakes analyses indicate that Takeda smallest loop model has an average time history to design displacement ratio almost equal to 1 while the largest loop model underestimates the displacements by about 20%. It is recommended to use the smallest loop model in displacement-based design for reinforced concrete members with ductility values less than 5, while the large loop model needs a reduction factor that will be a part of future work, which will also involve expanding the evaluation process to cover the Ring-Spring hysteretic model, which represents a self correcting system or seismic isolators, a bilinear model, and a strength degrading hysteretic model. A more advanced statistical analysis will be utilized to analyze the results and to obtain correction factors that account for: (1) oscillator period (2) level of damping (3) earthquake characteristics, and (4) and hysteretic model.

REFERENCES

1. Jacobsen L.S. "Steady Forced Vibrations as Influenced by Damping." ASME Transactione 1930, 52(1): 169-181.
2. Gulkan P. and Sozen M. "Inelastic Response of Reinforced Concrete Structures to Earthquake Motion." ACI Journal 1974, 71: 604-610.
3. Hudson D.E. "Equivalent Viscous Friction for Hysteretic Systems with Earthquake-Like Excitations." 3rd World Conference on Earthquake Engineering. New Zealand 1965, ppII-185/II-201

4. Shibata A. and Sozen M. “Substitute Structure Method for Seismic Design in R/C.” Journal of the Structural Division, ASCE 1976, 102(ST1): 1-18.

5. Kowalsky M.J., Priestley M.J.N. and McRae G.A. “Displacement Based Design of RC Bridge Columns in Seismic Regions.” Earthquake Engineering and Structural Dynamics 1995, 24(12): 1623-1643.

6. Iwan WD. “Estimating Inelastic Response Spectra from Elastic Spectra.” Earthquake Engineering and Structural Dynamics 1980, 8: 375-388.

7. Takeda T., Sozen M. and Nielsen N. “Reinforced Concrete Response to Simulated Earthquakes.” Journal of the Structural Division, ASCE 1970, 96(12): 2557-2573

8. Hill K.E. “Dynamic Properties of Ring Springs for Use as Seismic Energy Dissipaters.” Proceedings of NZSEE Technical Conference, Norway 1968.

9. Miranda E. Personal correspondence. Department of Civil and Environmental Engineering, Stanford University, CA.

10. Kowalsky M.J. and Ayers J.P. “Investigation of Equivalent Viscous Damping for Direct Displacement-Based Design.” The Third US-Japan Workshop on Performance-Based Earthquake Engineering Methodology for Reinforced Concrete Building Structures. Seattle, WA, August 2001.

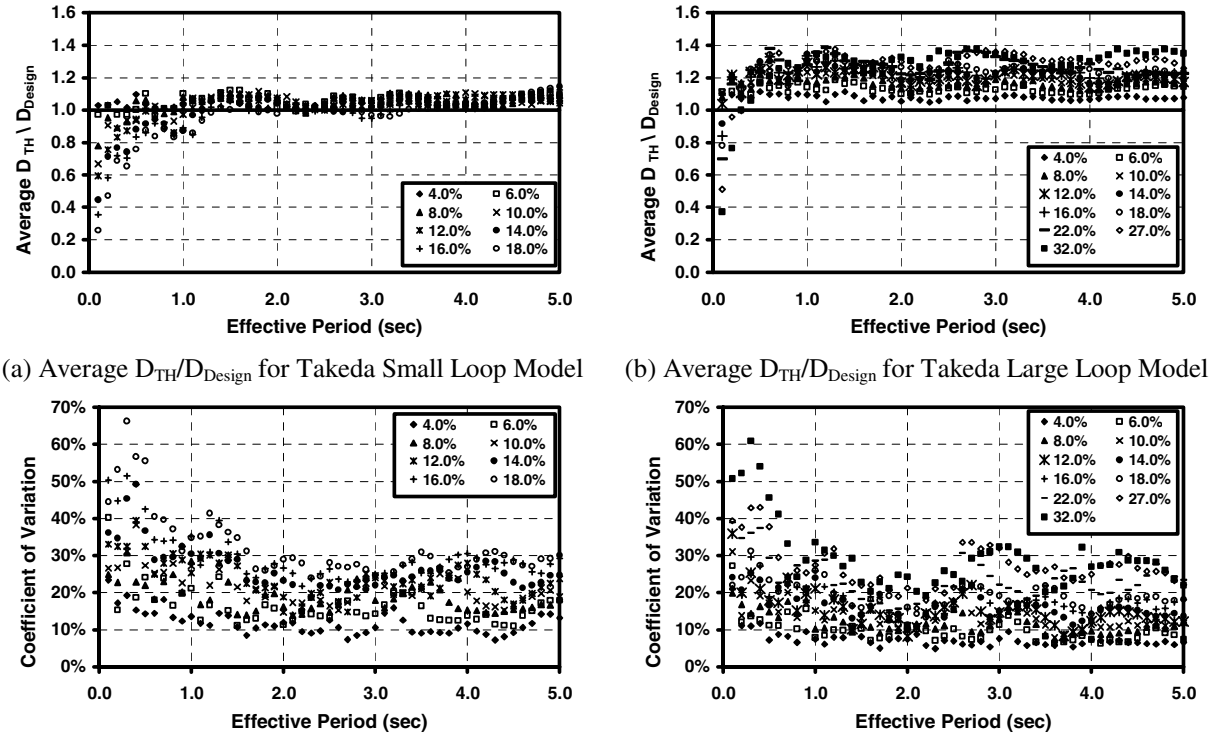

(a) Average D_{TH}/D_{Design} for Takeda Small Loop Model

(b) Average D_{TH}/D_{Design} for Takeda Large Loop Model

(c) CoV for Takeda Small Loop Model

(d) CoV for Takeda Large Loop Model

Figure 11 Average Time History to Design Displacement Ratio for Site B Earthquake Records

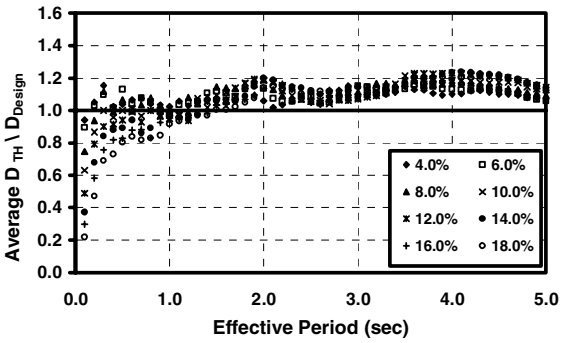

(a) Average D_{TH}/D_{Design} for Takeda Small Loop Model

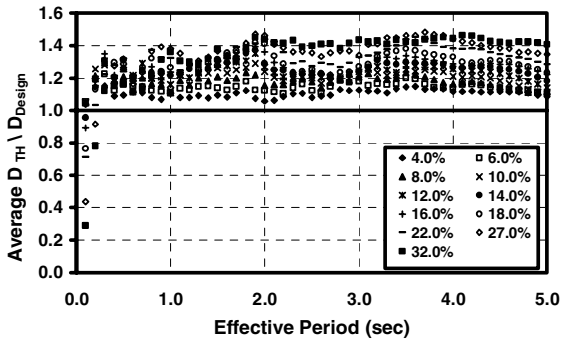

(b) Average D_{TH}/D_{Design} for Takeda Large Loop Model

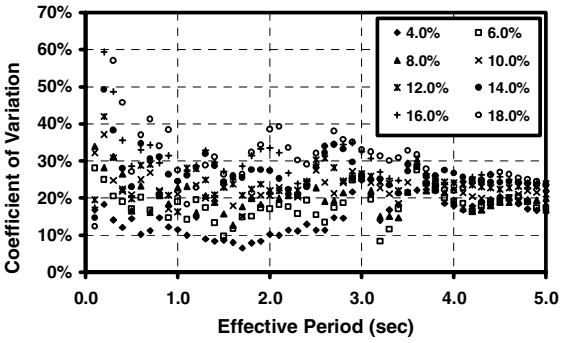

(c) CoV for Takeda Small Loop Model

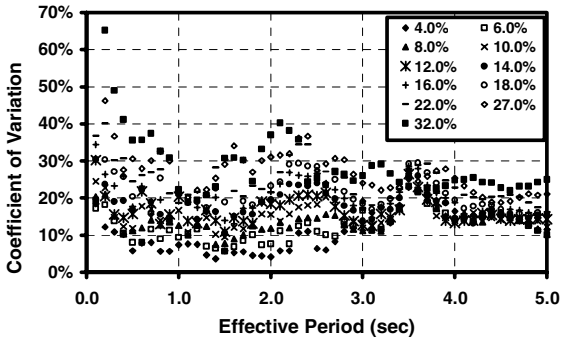

(d) CoV for Takeda Large Loop Model

Figure 12. Average Time History to Design Displacement Ratio for Site C Earthquake Records

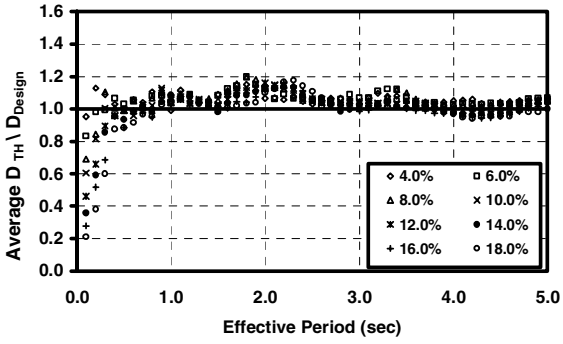

(a) Average D_{TH}/D_{Design} for Takeda Small Loop Model

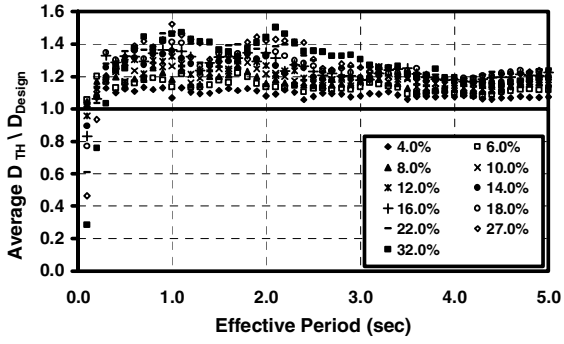

(b) Average D_{TH}/D_{Design} for Takeda Large Loop Model

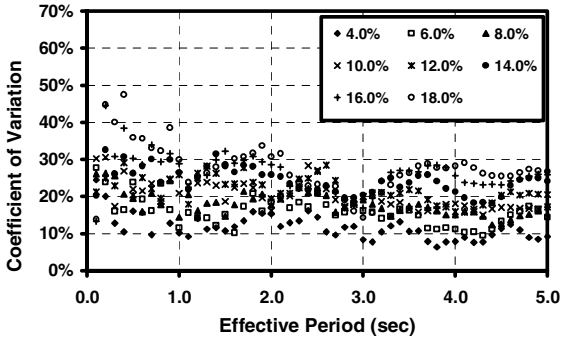

(c) CoV for Takeda Small Loop Model

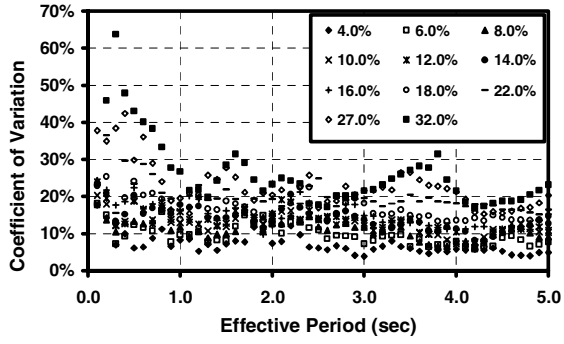

(d) CoV for Takeda Large Loop Model

Figure 13 Average Time History to Design Displacement Ratio for Site D Earthquake Records

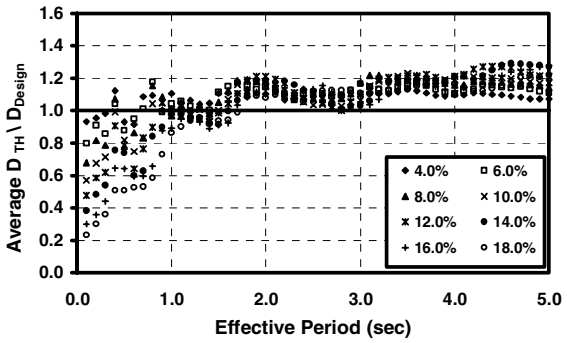

(a) Average D_{TH}/D_{Design} for Takeda Small Loop Model

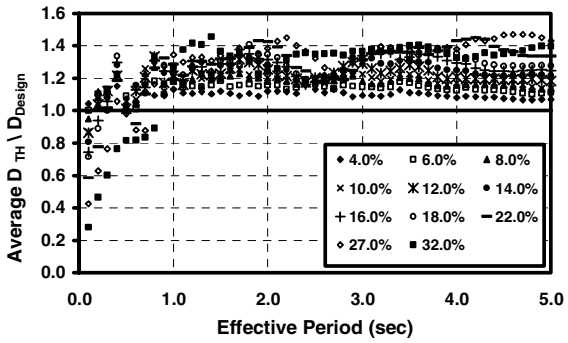

(b) Average D_{TH}/D_{Design} for Takeda Large Loop Model

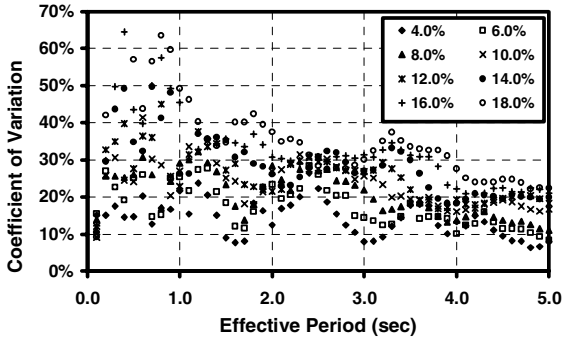

(c) CoV for Takeda Small Loop Model

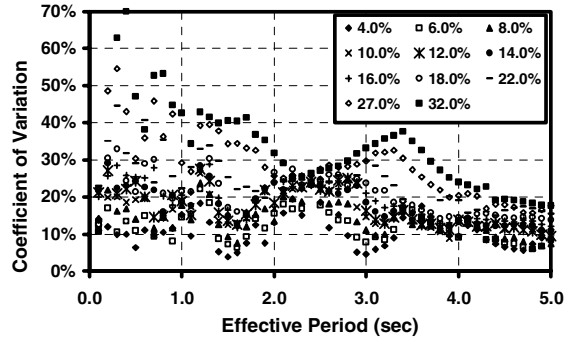

(d) CoV for Takeda Large Loop Model

Figure 13. Average Time History to Design Displacement Ratio for Site E Earthquake Records

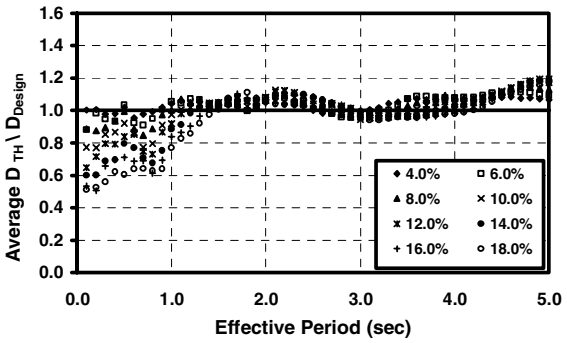

(a) Average D_{TH}/D_{Design} for Takeda Small Loop Model

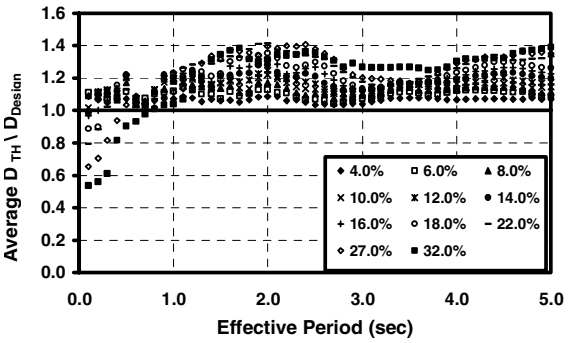

(b) Average D_{TH}/D_{Design} for Takeda Large Loop Model

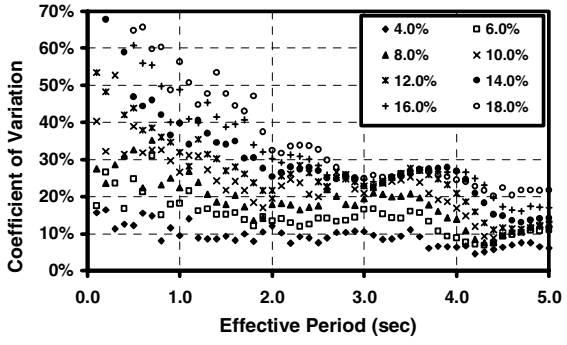

(c) CoV for Takeda Small Loop Model

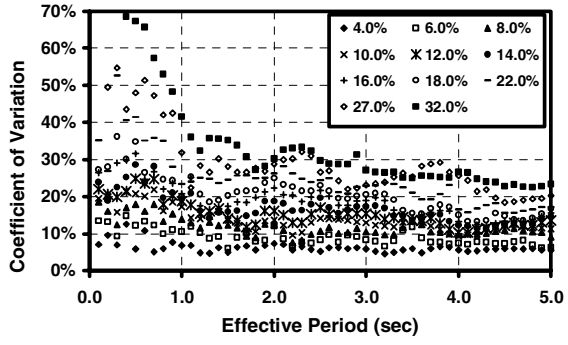

(d) CoV for Takeda Large Loop Model

Figure 14. Average Time History to Design Displacement Ratio for Site NF Earthquake Records